

Trusted Routing for Blockchain-Enabled Low-Altitude Intelligent Networks

Sijie He[†], Ziyi Jia[†], Qiuming Zhu[†], Fuhui Zhou[†], and Qihui Wu[†]

[†]The Key Laboratory of Dynamic Cognitive System of Electromagnetic Spectrum Space, Ministry of Industry and Information Technology, Nanjing University of Aeronautics and Astronautics, Nanjing, Jiangsu, 211106, China
{hesijie, jiaziye, zhuqiuming, zhoufuhui, wuqihui}@nuaa.edu.cn

Abstract—Due to the scalability and portability, the low-altitude intelligent networks (LAINs) are essential in various fields such as surveillance and disaster rescue. However, in LAINs, unmanned aerial vehicles (UAVs) are characterized by the distributed topology and high dynamic mobility, and vulnerable to security threats, which may degrade the routing performance for data transmission. Hence, how to ensure the routing stability and security of LAINs is a challenge. In this paper, we focus on the routing process in LAINs with multiple UAV clusters and propose the blockchain-enabled zero-trust architecture to manage the joining and exiting of UAVs. Furthermore, we formulate the routing problem to minimize the end-to-end (E2E) delay, which is an integer linear programming and intractable to solve. Therefore, considering the distribution of LAINs, we reformulate the routing problem into a decentralized partially observable Markov decision process. With the proposed soft hierarchical experience replay buffer, the multi-agent double deep Q-network based adaptive routing algorithm is designed. Finally, simulations are conducted and numerical results show that the total E2E delay of the proposed mechanism decreases by 22.38% than the benchmark on average.

Index Terms—Low-altitude intelligent networks, trusted routing, blockchain, soft hierarchical experience replay buffer, multi-agent deep reinforcement learning.

I. INTRODUCTION

As key components of the six generation communication networks, the low-altitude intelligent network (LAINs) are widely applied to multiple tasks, such as disaster rescue and real-time monitoring [1]–[3]. In these applications, the data generated from sensor devices (SDs) are required to be relayed to the remote ground base stations (BSs) by unmanned aerial vehicles (UAVs) [4]. Particularly, UAVs act as aerial relays and cooperatively accomplish the data collection and transmission, providing low-cost, flexible, and versatile services. In LAINs, routing is a significant issue for data transmission [5]–[7].

However, since UAVs in LAINs are characterized by the complex application environment, high mobility and distributed topology, they are vulnerable to security threats and unreliable, i.e., attacks and node failures. Thus, the availability of communication links is susceptible, which leads to the reduction of routing performances. Hence, it is significant to efficiently manage the mobility of UAVs in the zero-trust environment. There exist a couple of works

related to the management of UAVs. For instance, in [8], the ground control station (GCS) is responsible for managing the connection among all UAVs, through the status message sent by UAVs. In [9], the authors present that as the center controller and manager, the GCS receives the data transmitted by UAVs, which is suffered from long distances, undulating terrains or other interferences. Authors in [10] present that the GCS remotely controls UAVs by sending controlling information, in which the relay UAV is limited within the communication range of the GCS, restricting the scope of operations. Moreover, the above works rely on a center controller, which is not resilient to fault tolerance and may be susceptible to tampering. Hence, how to guarantee the reliability and security of routing remains challenging in the distributed and zero-trust network.

Meanwhile, the transmission delay is a key quality of service, since low delay can significantly improve the timeliness and reliability for various emergency applications, such as the surveillance information transmission [11]. Therefore, it is necessary to design an adaptive and dynamic algorithm to enable timely and reliable routing in the varying network topology. To tackle this issue, the multi-agent reinforcement learning (MARL) can be applied [12]. Specifically, there exist a couple of works focusing on MARL-based routing problems in dynamic scenarios. For example, in [13], the authors propose a value decomposition network based MARL algorithm to minimize the end-to-end (E2E) delay of packet routing within dynamic aerial and terrestrial hybrid networks. [14] formulates the packet routing as a max-min problem using the Lagrange method, and proposes a constrained MARL dynamic routing algorithm to balance the objective improvement and constraint satisfaction. Authors in [15] establish the mean-field enhanced heterogeneous MARL framework to optimize the communication energy efficiency during routing. The above studies illustrate that the MARL can solve the routing problem effectively. However, these works do not consider the mobility management of UAVs in the zero-trust environment.

To deal with the above challenges, in this paper, the routing process is depicted in the zero-trust LAINs with multiple UAV clusters, considering the dynamic joining and exiting of UAVs. Meanwhile, to improve the network reliability and security, the blockchain technique with a distributed ledger is introduced to manage the mobility of nodes and avoid being tempered with, by leveraging the smart contract. Further, a couple of UAVs with powerful capabilities are selected to

This work was supported in part by the Natural Science Foundation on Frontier Leading Technology Basic Research Project of Jiangsu under Grant BK20222001, in part by National Natural Science Foundation of China under Grant 62301251, in part by the Aeronautical Science Foundation of China 2023Z071052007, and in part by the Young Elite Scientists Sponsorship Program by CAST 2023QNRC001.

construct the decentralized controller in the blockchain. In light of the constructed LAIN, the routing problem is formulated to minimize the total E2E delay, which is an integer linear programming (ILP) and intractable to solve. Besides, it is tricky to obtain the global information due to decentralized UAVs. Hence, we reformulate the routing problem into a decentralized partially observable Markov decision process (Dec-POMDP). To improve the efficiency of learning and training, we propose the multi-agent double deep Q-network (MADDQN)-based adaptive routing approach with the designed soft hierarchical experience replay buffer (SHERB). Finally, numerical simulations are conducted to verify the performance of the proposed algorithm.

II. SYSTEM MODEL AND PROBLEM FORMULATION

A. Network Model

The routing process in zero-trust LAINs is shown in Fig. 1, including N nodes, and each node holds a unique identity. Specifically, when there exist UAVs applying to joining or exiting, the identities are authenticated and managed by smart contracts via the blockchain technique. Moreover, the periodical authentication is performed on all UAVs for the persistent verification. In detail, the ground layer consists of B BSs and I SDs. The air layer is composed of U UAVs. $\mathcal{B} = \{1, \dots, b, \dots, B\}$, $\mathcal{I} = \{1, \dots, i, \dots, I\}$, and $\mathcal{U} = \{1, \dots, u, \dots, U\}$ denote the sets of BSs, SDs, and UAVs, respectively. Besides, UAV set $\mathcal{U} = \mathcal{U}_s \cup \mathcal{U}_r \cup \mathcal{U}_d$ is divided based on clusters, in which \mathcal{U}_s , \mathcal{U}_r , and \mathcal{U}_d denote the data collection, relay forwarding, and downlinking clusters, respectively. In each cluster, the UAV with the most energy and computing power is selected as the cluster head. $\mathcal{E} = \mathcal{E}_{iu} + \mathcal{E}_{uu} + \mathcal{E}_{ub}$ indicates the set of communication link status among all nodes, where $e_{iu} \in \mathcal{E}_{iu}$, $e_{ub} \in \mathcal{E}_{ub}$, and $e_{uu} \in \mathcal{E}_{uu}$ represent the connection of links between the SD and UAV, the BS and UAV, and the UAV and UAV, respectively. $e_{nm} \in \mathcal{E}$ indicates whether there exists a communicable link between nodes $n \in \mathcal{I} \cup \mathcal{U}$ and $m \in \mathcal{U} \cup \mathcal{B}$. Specifically, $e_{nm} = 1$ indicates the link is effective, and $e_{nm} = 0$ denotes there exist no direct links.

In particular, the time period is divided into T steps. The set of time steps is represented as $T = \{1, \dots, t, \dots, T\}$. At the beginning of time step t , demand r is transmitted from SD $i \in \mathcal{I}$ to destination BS $b \in \mathcal{B}$, denoted by $\mathcal{R}^r = \{s^r, \mathcal{L}^r, d^r, \mathcal{T}_{max}^r\}$, in which the source is $s^r = i$, and the destination is $d^r = b$. Here, the size of demand r is \mathcal{L}^r (in bit), and \mathcal{T}_{max}^r is the maximum delay tolerance of the demand transmission. Further, demands are uploaded from SD $i \in \mathcal{I}$ to UAV $u \in \mathcal{U}_s$, relayed by UAV $u \in \mathcal{U}_r$, and downloaded from UAV $u \in \mathcal{U}_d$ to BS $b \in \mathcal{B}$. $\mathcal{P}_{ib}^r = (e_{iu}, \dots, e_{ub})$ indicates a completed routing path for transmitting demand r .

The coordinates of SD i and BS b remain fixed and are $\Theta_i = (x_i, y_i, 0)$ and $\Theta_b = (x_b, y_b, 0)$, respectively. The location of UAV u is indicated by $\Theta_u(t) = (x_u(t), y_u(t), z_u(t))$ in three-dimensional Cartesian coordinates at time step t . Additionally, the Euclidean distance between nodes $n \in \mathcal{I} \cup \mathcal{U}$ and $m \in \mathcal{U} \cup \mathcal{B}$ is indicated by $d_{nm}(t)$ at time step t , i.e.,

$$d_{nm}(t) = \sqrt{(x_n(t) - x_m(t))^2 + (y_n(t) - y_m(t))^2 + (z_n(t) - z_m(t))^2}. \quad (1)$$

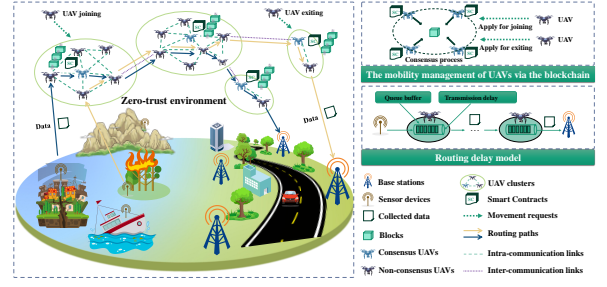


Fig. 1. Routing scenario in zero-trust LAINs with the mobility management of UAVs via the blockchain technique.

In particular, the distance between UAVs should satisfy

$$d_{min} \leq d_{nm}(t), \forall n, m \in \mathcal{U}, n \neq m, t \in T. \quad (2)$$

Here, d_{min} represents the safe distance to avoid collisions among UAVs. At time step t , the set of connected UAVs for UAV u is denoted as $\Gamma_u(t)$, and distance $d_{u\kappa}(t)$ between UAV u and UAV $\kappa \in \Gamma_u(t)$ satisfies

$$d_{u\kappa}(t) \leq d_{u,max}, \forall \kappa \in \Gamma_u(t), u \in \mathcal{U}, t \in T, \quad (3)$$

in which $d_{u,max}$ is the maximum communication distance of UAV u .

B. Blockchain Model

To manage the mobility of UAVs, a lightweight blockchain model is proposed. Additionally, to maintain the sustainability and reliability of routing, the joining and exiting of UAVs need to be recorded and updated via the blockchain.

1) *Role Selection*: In the lightweight blockchain, the set \mathcal{U} of UAVs is divided into the sets of full nodes $\mathcal{U}_f = \{1, 2, \dots, u_f\}$ and light nodes $\mathcal{U}_l = \{1, 2, \dots, u_l\}$, respectively. In detail, as shown in Fig. 1, cluster head UAVs are selected as full nodes due to the sufficient resources, while the other UAVs act as light nodes in LAINs. In particular, the full nodes have the full blockchain ledger and are responsible for the blockchain consensus, including broadcasting and verification of transactions. The light nodes can only store the header of blocks and are in charge of generating local transactions and relaying transactions from other UAVs.

2) *PBFT-based Consensus Process*: We apply the practical Byzantine fault tolerance (PBFT) method, which can ensure the success of the consensus process when the number of failure nodes is less than one third. For the effectiveness and reliability of the PBFT consensus, it is significant to select consensus UAVs with the most abundant resources as the primary node, while other consensus UAVs operate as non-primary (replica) nodes.

3) *Transaction Generation and Broadcasting*: The transactions waiting for the consensus are generated periodically and include the status of UAVs, i.e., the queue buffer, location, and information of neighboring nodes. Then, all generated transactions are broadcasted to the entire network via the Gossip protocol for verifying. After verification, the transactions are added to the transaction pool of the blockchain and then synchronized to the entire blockchain. Once a consensus is reached, the data transaction is recorded in the blockchain with tamper-proof.

C. Delay Model

As shown in Fig. 1, in LAINs, the E2E routing delay consists of the total transmission delay on the multi-hop path from the source UAV to destination UAV. Since the delay is constrained by data transmission rate G , it is essential to analyze the channel characteristics of both ground-to-air and air-to-air wireless communication links.

Regard to demand r , binary variable $\zeta_n^r(t) \in \{0, 1\}$ clarifies the transmission status, i.e.,

$$\zeta_n^r(t) = \begin{cases} 1, & \text{if } r \text{ is on node } n \in \mathcal{I} \cup \mathcal{U} \text{ at time step } t, \\ 0, & \text{otherwise.} \end{cases} \quad (4)$$

Besides, binary variable $\eta_{nm}^r(t) \in \{0, 1\}$ denotes whether demand r passes link e_{nm} ($n \in \mathcal{I} \cup \mathcal{U}, m \in \mathcal{U} \cup \mathcal{B}$), i.e.,

$$\eta_{nm}^r(t) = \begin{cases} 1, & \text{if } r \text{ is transmitted via } e_{nm} \text{ at time step } t, \\ 0, & \text{otherwise.} \end{cases} \quad (5)$$

Further, $L_{nm}(t)$ is the path loss between nodes $n \in \mathcal{I} \cup \mathcal{U}$ and $m \in \mathcal{U} \cup \mathcal{B}$ and remains constant within time step t , i.e.,

$$L_{nm}(t) = 20 \log \left(\frac{4\pi\lambda}{c} d_{nm}(t) \right) + \omega [\Pr_{nm}(t) (\eta_{nm}^{\text{LoS}}(t) - \eta_{nm}^{\text{NLoS}}(t)) + \eta_{nm}^{\text{NLoS}}(t)], \quad (6)$$

where $\eta_{nm}^{\text{LoS}}(t)$ and $\eta_{nm}^{\text{NLoS}}(t)$ represent the additional path losses under LoS and non-LoS (NLoS) propagations, respectively. When $\omega = 1$, $L_{nm}(t)$ is the path loss from $n \in \mathcal{I}$ to $m \in \mathcal{U}$ or $n \in \mathcal{U}$ to $m \in \mathcal{B}$. While $\omega = 0$, $L_{nm}(t)$ indicates the path loss between UAVs. λ represents the carrier frequency, and c is the speed of light. Besides, $\Pr_{nm}(t)$ indicates the probability that there exist line of sight (LoS) links between SDs/BSs and UAVs, i.e.,

$$\Pr_{nm}(t) = \frac{1}{1 + \varrho_1 \exp \left\{ -\varrho_2 \left[\frac{180}{\pi} \arctan \left(\frac{h_{nm}(t)}{xy_{nm}(t)} \right) - \varrho_1 \right] \right\}}, \quad (7)$$

in which ϱ_1 and ϱ_2 are the constant parameters [16].

Since LAINs are characterized by high mobility and unstable data traffic fluctuations, we introduce a queue buffer for each node $n \in \mathcal{I} \cup \mathcal{U}$ to alleviate the network congestion. In particular, for node n , the amount of demands received at time step $t-1$ is $\varepsilon_n^{re}(t-1)$. At time step t , the queued demand set, queue length, maximum queue capacity, and the number of transmitted demands of node n are denoted as $C_n(t) = \{r, \zeta_n^r(t) = 1, \forall r \in R\}$, $C_n(t)$, C_n^{\max} , and $\varepsilon_n^{tr}(t)$, respectively. In detail,

$$\begin{cases} \varepsilon_n^{re}(t-1) = \sum_{r \in R} \sum_{m \in \mathcal{I} \cup \mathcal{U}} \eta_{mn}^r(t-1), 0 \leq \varepsilon_n^{re}(t-1) \leq C_n^{\max}, \\ C_n(t) = \sum_{r \in R} \zeta_n^r(t), 0 \leq C_n(t) \leq C_n^{\max}, C_n(t) = |C_n(t)|, \\ \varepsilon_n^{tr}(t) = \sum_{r \in C_n(t)} \sum_{m \in \mathcal{U} \cup \mathcal{B}} \eta_{nm}^r(t), \varepsilon_n^{tr}(t) = C_n(t). \end{cases} \quad (8)$$

Here, the UAV leverages the parallel transmission for demands, indicating that UAVs forward all demands received from the last time step. Besides, the adaptive channel bandwidth allocation scheme is designed to narrow the transmission delay gap of different demands in one time step. Hence,

at time step t , the allocated bandwidth $B_n^r(t)$ is calculated based on the size of demand $r \in C_n(t)$, i.e.,

$$B_n^r(t) = \frac{\mathcal{L}^r}{\sum_{k \in C_n(t)} \mathcal{L}^k} B_n(t), \forall n \in \mathcal{I} \cup \mathcal{U}, r \in C_n(t), t \in T, \quad (9)$$

where $B_n(t)$ is the total bandwidth of node n at time step t . Based on Shannon theory, at time step t , transmission rate $G_{nm}^r(t)$ for demand r from nodes $n \in \mathcal{I} \cup \mathcal{U}$ to $m \in \mathcal{U} \cup \mathcal{B}$ is

$$G_{nm}^r(t) = B_n^r(t) \log_2 \left(1 + \frac{P_{nm}^{tr}(t) \cdot 10^{-\frac{L_{nm}(t)}{10}}}{\sigma_{nm}^2(t)} \right), r \in C_n(t), \quad (10)$$

where $P_{nm}^{tr}(t)$ and $\sigma_{nm}^2(t)$ indicate the transmission power and noise power between nodes n and m , respectively. Then, the transmission delay for demands from nodes n to m is

$$\mathcal{T}_{nm}^{tr,r}(t) = \max_{r \in R} \frac{\mathcal{L}^r}{G_{nm}^r(t)} \eta_{nm}^r(t), \quad \forall r \in R, n \in \mathcal{I} \cup \mathcal{U}, m \in \mathcal{U} \cup \mathcal{B}, t \in T. \quad (11)$$

When the routing path \mathcal{P}_{ib}^r for transmitting demand r from source SD i to destination BS b is determined, E2E delay \mathcal{T}^r can be calculated as

$$\mathcal{T}^r = \sum_{t \in T} \sum_{e_{nm} \in \mathcal{P}_{ib}^r} \mathcal{T}_{nm}^{tr,r}(t), \forall r \in R, n \in \mathcal{I} \cup \mathcal{U}, m \in \mathcal{U} \cup \mathcal{B}. \quad (12)$$

D. Problem Formulation

The objective is to minimize the total E2E delay of LAINs with the mobility of nodes, and the corresponding optimization problem is formulated as

$$\begin{aligned} \mathcal{P}0 : \min_{\eta, \zeta} \quad & \mathcal{T}^r \\ \text{s.t.} \quad & (2), (3), (4), (5), (8), \\ & \sum_{m \in \mathcal{U} \cup \mathcal{B}} \eta_{nm}^r(t) = 1, \forall r \in R, t \in T, e_{nm} \in \mathcal{E}, \\ & \forall n \in \mathcal{I} \cup \mathcal{U}, m \in \mathcal{U} \cup \mathcal{B}, \end{aligned} \quad (13)$$

where $\eta = \{\eta_{nm}^r(t), \forall t \in T, e_{nm} \in \mathcal{E}, n \in \mathcal{I} \cup \mathcal{U}, m \in \mathcal{U} \cup \mathcal{B}, r \in R\}$, and $\zeta = \{\zeta_n^r(t), \forall t \in T, n \in \mathcal{I} \cup \mathcal{U}, r \in R\}$. Besides, the demand r from node $n \in \mathcal{I} \cup \mathcal{U}$ can only be received by one another node $m \in \mathcal{U} \cup \mathcal{B}$. It is observed that $\mathcal{P}0$ is in the form of ILP and NP-hard to deal with [17].

III. PROBLEM FORMULATION AND ALGORITHM DESIGN

A. Dec-POMDP based Reformulation

Since each UAV has a local observation rather than global observation, $\mathcal{P}0$ is reformulated as a Dec-POMDP, to cater for the dynamically changing network environment. Each UAV in LAINs is regarded as an independent agent and makes its own routing decision that sends a demand to an alternative next UAV. Hence, the set of all agents is equal to UAV set \mathcal{U} . At each time step t , agent $u \in \mathcal{U}$ observes local state $o_u(t)$ of the environment and executes action $a_u(t)$ according to the observable state. Then, agent u receives an immediate reward $\mathcal{R}_u(t+1)$, and the environment is transferred to next observation state $o_u(t+1)$. The tuple

$\langle o_u(t), a_u(t), \mathcal{R}_u(t), o_u(t+1), f_u(t) \rangle$ indicates the transition experience of agent u and is explained in detail.

- State space \mathcal{S} : At time step t , the observable state $o_u(t)$ of agent u includes the available information of the current UAV and neighboring UAVs, detailed as

$$o_u(t) = \{\Theta_u(t), \mathcal{C}_u(t), \Theta_\kappa(t), \mathcal{C}_\kappa(t)\}, \kappa \in \Gamma_u(t). \quad (14)$$

Wherein, $\Theta_u(t)$ and $\Theta_\kappa(t)$ indicate the locations of UAV u and neighbor UAV κ , respectively. $\mathcal{C}_u(t)$ and $\mathcal{C}_\kappa(t)$ are the set of queued demands on UAVs u and κ , respectively. The queued demand set includes the information tuple \mathcal{T}^r of each demand r . The observations of all agents are aggregated into joint state $s(t)$ in time step t , denoted as $s(t) = \{o_u(t), u \in \mathcal{U}\}$, and the state space is indicated as $\mathcal{S} = \{s(t) | t \in T\}$.

- Action space \mathcal{A} : Agent u makes decisions for each carried demand independently, and the set $a_u(t) = \{a_u^r(t), r \in \mathcal{C}_u(t)\}$ represents the actions for demand $r \in \mathcal{C}_u(t)$ at time step t . Wherein, each sub-action $a_u^r(t)$ denotes the next-hop neighboring node selected by UAV u to relay demand r , i.e.,

$$\begin{cases} a_u^r(t) \in \{\Gamma_u(t)\}, u \in \mathcal{U}_s \cup \mathcal{U}_r, \\ a_u^r(t) \in \{\Gamma_u(t), Z_u(t)\}, u \in \mathcal{U}_d, \end{cases} \quad (15)$$

where $Z_u(t)$ is the set of BSs connected with UAV $u \in \mathcal{U}_d$ at time step t . If the destination BS b of demand $r \in \mathcal{C}_u(t)$ connects to UAV $u \in \mathcal{U}_d$, the demand is directly transmitted to destination b by UAV u . On the contrary, the demand is relayed by neighboring UAVs. The actions of all agents are aggregated as $\mathbf{a}(t) = \{a_u(t), u \in \mathcal{U}\}$ in time step t , and the action space is $\mathcal{A} = \{\mathbf{a}(t) | t \in T\}$.

- Reward \mathcal{R} : $\mathcal{R}_u(t) = \{\mathcal{R}_u^r(t) | r \in \mathcal{C}_u(t)\}$, where $\mathcal{R}_u^r(t)$ is the reward that agent u obtains after transmitting demand r to neighboring node κ at time step t , i.e.,

$$\mathcal{R}_u^r(t) = \frac{1}{\mathcal{T}_{u\kappa}^{tr,t}(t)} \eta_{u\kappa}^r(t), \forall r \in \mathcal{C}_u(t), \kappa \in \Gamma_u(t). \quad (16)$$

- Transition flag \mathbf{f} : $\mathbf{f}(t) = \{f^r(t) | r \in \mathcal{C}_u(t)\}$, where $f^r(t)$ indicates whether demand r arrives at destination BS $b \in \mathcal{B}$, defined as

$$f^r(t) = \begin{cases} 1, & \text{if } a_u^r(t) \text{ is the destination BS } b, \\ 0, & \text{otherwise.} \end{cases} \quad (17)$$

- Discount factor γ : $\gamma = \{\gamma_u | u \in \mathcal{U}\}$, in which γ_u is designed to calculate the cumulative reward. A larger γ indicates decisions focusing on the long-term reward.

The policy $\pi_u^r(t)$ leads agent u to select action $a_u^r(t)$ for demand r under observation $o_u(t)$ at time step t . $\pi_u(t) = \{\pi_u^r(t), \forall r \in \mathcal{C}_u(t)\}$ indicates the joint policy of all demands on agent u . $\Pi(t) = \{\pi_u(t), \forall u \in \mathcal{U}\}$ indicates the policy of all agents. According to the Dec-POMDP and specific policy $\Pi(t)$, we can obtain the routing path for all demands. Therefore, $\mathcal{P}0$ is transformed to find the optimal policy $\Pi^*(t) = \{\pi_u^*(t), \forall u \in \mathcal{U}\}$, and then the improved MADRL-based routing method is designed to obtain $\Pi^* = \{\Pi^*(t) | t \in T\}$ for minimizing the total E2E delay.

B. SHERB-MADDQN-based Routing Algorithm

In dynamic scenarios with multiple sources and destinations, to improve the learning efficiency of routing strategies, the adaptive SHERB-MADDQN-based routing algorithm is designed. In detail, the experience buffer of each agent is softly constructed by embedding the state information of the destination BS in the reward. Thus, the reward in (16) is reformulated as

$$\mathcal{R}_u^r(t) = \frac{1}{\mathcal{T}_{u\kappa}^{tr,t}(t) + \varsigma} \cdot \frac{d_{u\kappa}(t)}{d_{u\kappa}(t) + d_{\kappa b}(t)} \eta_{u\kappa}^r(t), \quad (18)$$

$$r \in \mathcal{C}_u(t), \kappa \in \Gamma_u(t), t \in T,$$

where $d_{u\kappa}(t)$ and $d_{\kappa b}(t)$ denote distances from UAV u to neighboring UAV κ , and from UAV κ to destination BS b , respectively. ς is a hyperparameter to balance the benefits from the delay and distance. It is noted that $d_{u\kappa}(t)$ is positively related to the reward, since a larger value of $d_{u\kappa}(t)$ indicates a fewer hop counts required, saving time in queuing for transmission. Meanwhile, $d_{u\kappa}(t) + d_{\kappa b}(t)$ represents the total transmission distance from the selected next hop κ to UAV u and BS b . If $d_{u\kappa}(t) + d_{\kappa b}(t)$ is closer to the straight shortest distance between UAV u and BS b , agent u may obtain the greater value of rewards, and vice versa. Moreover, compared with the hard-HERB (HHERB)-based method that constructs a hierarchical data structure to store the experience, the SHERB can mitigate the problem of sparse experience samples, improving the sample utilization efficiency and generalization ability of strategies.

Furthermore, when the dimensions of state and action spaces are large, it is tricky to maintain the Q-table in Q-learning. Besides, the deep Q-network (DQN)-based algorithm may cause a large deviation caused by overestimating the Q-target value. Hence, by combining double Q-learning with DQNs, DDQN algorithms are proposed to approximate Q-value functions via deep neural networks (DNNs) and decouple the action selection and calculation of Q-target values [18]. Further, for the DDQN, there exist two DNNs, i.e., the online network with parameter θ_u and the target network with parameter θ_u^- of each agent u . Through constantly updating the weight θ_u of online networks, loss function $L(\theta_u)$ is trained and then minimized. The experience replay buffer (ERB) of agent u is designed to store the historical experience and denoted as $\mathcal{D}_u = \{(o_u(t), a_u^r(t), \mathcal{R}_u^r(t+1), o_u(t+1)) | r \in \mathcal{C}_u(t)\}$. By randomly sampling D transition tuples from \mathcal{D}_u , $L(\theta_u)$ is typically computed as the mean squared error between Q-value function $Q(o_u(t), a_u(t); \theta_u)$ and Q-target $y_u(t)$, i.e.,

$$L(\theta_u) = \mathbb{E}_{\xi \sim \mathcal{D}_u} [(y_u(t) - Q(o_u(t), a_u(t); \theta_u))^2], \quad (19)$$

where tuple ξ is a transition data of \mathcal{D}_u , and $y_u(t)$ is

$$y_u(t) = \mathcal{R}_u(t+1) + \gamma_u Q(o_u(t+1), \arg \max_{a_u^r(t)} Q(o_u(t+1), a_u^r(t); \theta_u^-) | \theta_u^-). \quad (20)$$

Besides, the gradient of $L(\theta_u)$ is denoted as $\nabla_{\theta_u} L(\theta_u)$, which is used to update θ_u via the gradient descent, i.e.,

$$\theta_u \leftarrow \theta_u - \alpha_u \nabla_{\theta_u} L(\theta_u). \quad (21)$$

Algorithm 1 SHERB-MADDQN-based routing algorithm**Input:** $\mathcal{I}, \mathcal{U}, \mathcal{B}, \mathcal{E}, R, \alpha$, and γ .**Output:** Optimal policy Π^* .

```

1: Initialization: Initialize the network environment, hyper-
   parameters, ERB set  $\mathcal{D}$ , and the online and target
   network parameters  $\theta_u$  and  $\theta_u^-$  for each agent  $u \in \mathcal{U}$ ,
   respectively.
2: for each episode do
3:   for  $t = 1, \dots, T$  do
4:     for  $u = 1, \dots, U$  do
5:       The observation of agent  $u$  is set as  $o_u(t)$ .
6:       Allocate the bandwidth based on queued demands
       in  $\mathcal{C}_u(t)$  via (9).
7:       for  $r = 1, \dots, |\mathcal{C}_u(t)|$  do
8:         Select action  $a_u^r(t)$  for demand  $r$  under obser-
         vation  $o_u(t)$  using an  $\epsilon$ -greedy policy.
9:         Execute  $a_u^r(t)$ , and obtain reward  $\mathcal{R}_u^r(t+1)$ .
10:      end for
11:      if  $|\mathcal{D}_u| > D$  then
12:        Randomly select  $D$  samples from  $\mathcal{D}_u$ .
13:        Compute Q-target value  $y_u(t)$  via (20).
14:        Update  $\theta_u$  via the gradient descent in (21).
15:        Periodically update target network parameter
         $\theta_u^-$  via (22) every  $\mathcal{W}$  steps.
16:      end if
17:    end for
18:    Update the environment, and set observation
     $o_u(t) \leftarrow o_u(t+1)$  for all agents in  $\mathcal{U}$ .
19:    Store transition  $(o_u(t), a_u^r(t), \mathcal{R}_u^r(t+1), o_u(t+1))$ 
    of each demand  $r$  into corresponding  $\mathcal{D}_u$ .
20:  end for
21: end for

```

Wherein, α_u is the learning rate that controls the size of update steps. In every \mathcal{W} steps, parameter θ_u^- is periodically updated to match the parameter of online network θ_u for stabilizing training and improving the convergence, i.e.,

$$\theta_u^- \leftarrow \tau \theta_u + (1 - \tau) \theta_u^-, \quad (22)$$

where τ is the soft update coefficient.

The detail of the proposed SHERB-MADDQN-based routing method is shown in Algorithm 1. Firstly, the algorithm initializes the network environment, hyper-parameters, ERB set \mathcal{D} , and the parameters of DNNs, respectively (line 1). At the beginning of each episode, the observation of agent u is initialized as $o_u(t)$ (lines 2-5). Then, according to (9), the bandwidth of agent u is allocated according to queued demands in $\mathcal{C}_u(t)$ (line 6). Based on $o_u(t)$, each agent u selects sub-action $a_u^r(t)$ for demand r via an ϵ -greedy policy, and then executes $a_u^r(t)$ to obtain reward $\mathcal{R}_u^r(t+1)$ (lines 7-10). If the number of transition tuples in \mathcal{D}_u is larger than mini-batch D , D samples are randomly selected to calculate Q-target value $y_u(t)$ via (20) (lines 11-13). Additionally, the DNN performs a gradient descent step to update θ_u (line 14). The target network parameter θ_u^- is periodically updated according to (22) every \mathcal{W} steps (line 15). At time step t , when all agents finish the actions of all demands, the environment is updated. Further, each agent $u \in \mathcal{U}$ obtains

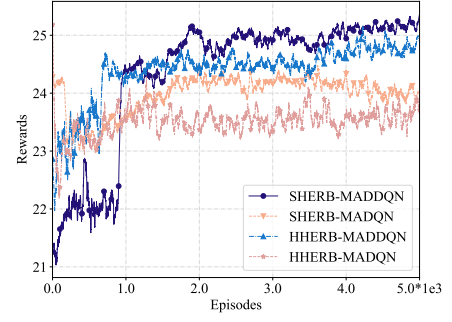


Fig. 2. Comparisons of the four algorithms in terms of the accumulative reward during the training process.

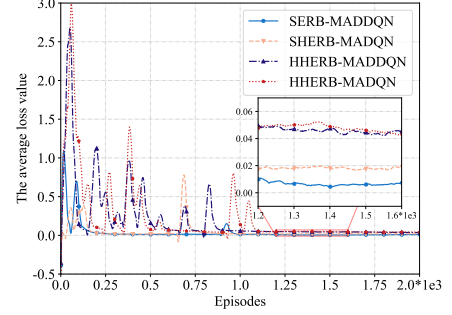


Fig. 3. Comparisons of the four algorithms in terms of the convergence performance during the training process.

next observation $o_u(t+1)$ to update observation $o_u(t)$ (line 18). Besides, the transition $(o_u(t), a_u^r(t), \mathcal{R}_u^r(t+1), o_u(t+1))$ of each demand r is stored into corresponding \mathcal{D}_u for training (line 19).

IV. SIMULATION RESULTS

In this section, a couple of simulations are conducted via Python. Specifically, nodes of LAINs are distributed in the area within a $15\text{km} \times 5\text{km}$ range, the altitude range of UAVs is within $[0.2, 0.4]\text{km}$. UAVs are initialized by the ground control center at the beginning of missions. Besides, the size of demands from SDs is randomly set within $[400, 600]\text{kbits}$. Other parameters are set as: $d_{\min} = 10\text{m}$, $d_{u,\max} = 100\text{m}$, $\sigma_{ij}^2 = -110\text{dBm}$, $\lambda = 2.4\text{GHz}$, $c = 3 \times 10^8\text{m/s}$, $P^{\text{tr}} = 40\text{dBm}$, $C_i^{\max} = 50$, $B_u = 2\text{MHz}$, $\varrho_1 = 5.0188$, $\varrho_2 = 0.3511$, $\eta_{nm}^{\text{LoS}} = 0.1\text{dB}$, and $\eta_{nm}^{\text{LoS}} = 21\text{dB}$ [?], [19].

To demonstrate the performance of Algorithm 1, different metrics are evaluated by comparing with SHERB-MADQN, HHERB-MADDQN, and HHERB-MADQN algorithms in Figs. 2-5. Specifically, in Fig. 2, the accumulative rewards are provided to evaluate the convergence performance. It can be observed that all four algorithms converge with different performances. In the first 2,000 episodes, rewards are not satisfactory. As the number of episodes increases, rewards increase and converge at the specific values. Besides, the rewards of SHERB-MADRL-based methods are larger compared to the rewards of HHERB-MADRL-based algorithms, due to the higher learning efficiency of the proposed SHERB. Meanwhile, the convergence value of the proposed SHERB-MADDQN algorithm is larger than the SHERB-MADQN algorithm. Hence, according to the designed (16) where rewards are negative, the proposed algorithm may have less delay for routing. In Fig. 3, the loss functions of all four

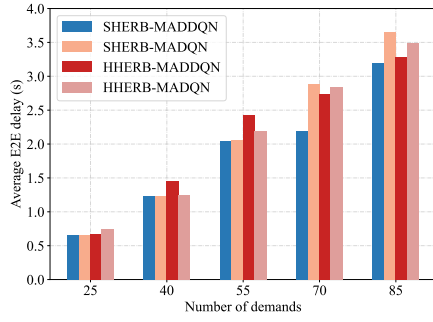


Fig. 4. Comparisons of the four algorithms in terms of average E2E delay.

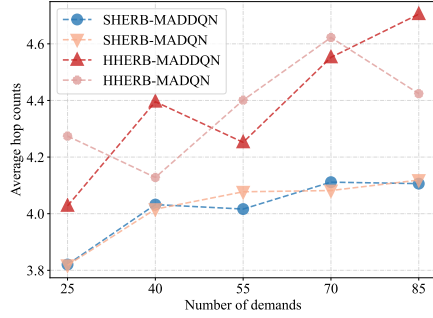


Fig. 5. Comparisons of the four algorithms in terms of average hop counts.

algorithms converge. For the proposed SHERB-MADDQN, the convergence speed is faster and the curve fluctuation of loss functions has a narrower range. Moreover, the loss value of the proposed method is smaller compared to other algorithms when the curve converges, indicating a more stable and effective training process.

The E2E delay for transmitting demands is evaluated in Fig. 4. It is observed that as demands grow, the E2E delay of the data transmission increases for all algorithms, due to the limited resources of the bandwidth. Nevertheless, the delay of the SHERB-MADDQN algorithm decreases by 24.09%, 20.49%, and 22.56% than the delay of SHERB-MADQN, HHERB-MADDQN, and HHERB-MADQN algorithms, respectively. Fig. 5 shows the performance of hop counts under different demand numbers. Specifically, with the increasing demands, the average hop counts of all algorithms grow, due to the increased congestion of networks. Nevertheless, the SHERB-based algorithm requires fewer hop counts for transmitting demands, benefiting from the better training performance of the algorithm. In short, simulation results demonstrate that the proposed algorithm performs better during routing.

V. CONCLUSIONS

In this work, we characterize the routing process of multiple sources and destinations in zero-trust LAINs, with the joining and exiting of UAVs. Additionally, the blockchain technique is introduced to manage the mobility and verify identities, enhancing the reliability and safety during routing. Besides, the routing problem is formulated to minimize the total E2E delay with multi-constraints. Further, we reformulate the routing problem into a Dec-POMDP to deal with the challenge of obtaining global information in LAINs characterized by the high dynamic, distributed topology. Then, to

improve the learning efficiency of the MARL, a SHERB-MADDQN-based algorithm is proposed via embedding the observed state into rewards. Simulation results in LAINs demonstrate that the designed SHERB-MADDQN algorithm outperforms in the delay, convergence, and loss value of training performances than other algorithms.

REFERENCES

- [1] B. He, X. Ji, G. Li, and B. Cheng, "Key technologies and applications of UAVs in underground space: A review," *IEEE Trans. Cognit. Commun. Networking*, vol. 10, no. 3, pp. 1026–1049, Jan. 2024.
- [2] Z. Jia, J. You, C. Dong, Q. Wu, F. Zhou, D. Niyato, and Z. Han, "Cooperative cognitive dynamic system in uav swarms: Reconfigurable mechanism and framework," *IEEE Veh. Technol. Mag.*, vol. 19, no. 3, pp. 90–101, Sep. 2024.
- [3] Z. Jia, C. Cui, C. Dong, Q. Wu, Z. Ling, D. Niyato, and Z. Han, "Distributionally robust optimization for aerial multi-access edge computing via cooperation of uavs and haps," *IEEE Trans. Mob. Comput.*, 2025, early access.
- [4] Z. Jia, Y. Cao, L. He, Q. Wu, Q. Zhu, D. Niyato, and Z. Han, "Service function chain dynamic scheduling in space-air-ground integrated networks," *IEEE Trans. Veh. Technol.*, 2025, early access.
- [5] D. Shumaye Lakew, U. Sa'ad, N.-N. Dao, W. Na, and S. Cho, "Routing in flying ad hoc networks: A comprehensive survey," *IEEE Commun. Surv. Tutorials*, vol. 22, no. 2, pp. 1071–1120, 2nd Quart. 2020.
- [6] S. He, Z. Jia, C. Dong, W. Wang, Y. Cao, Y. Yang, and Q. Wu, "Routing recovery for UAV networks with deliberate attacks: A reinforcement learning based approach," in *Proc. IEEE Glob. Commun. Conf.*, Kuala Lumpur, Malaysia, Dec. 2023, pp. 952–957.
- [7] Y. Ke, K. Huang, X. Qiu, B. Song, L. Xu, J. Yin, and Y. Yang, "Distributed routing optimization algorithm for FANET based on multi-agent reinforcement learning," *IEEE Sens. J.*, vol. 24, no. 15, pp. 24 851–24 864, Aug. 2024.
- [8] D. J. S. Agron, M. R. Ramli, J.-M. Lee, and D.-S. Kim, "Secure ground control station-based routing protocol for UAV networks," in *Proc. Int. Conf. Inf. Commun. Technol. Converg. (ICTC)*, Oct. 2019, pp. 794–798.
- [9] D. Yin, X. Yang, H. Yu, S. Chen, and C. Wang, "An air-to-ground relay communication planning method for UAVs swarm applications," *IEEE Trans. Intell. Veh.*, vol. 8, no. 4, pp. 2983–2997, Apr. 2023.
- [10] Y. Chen, G. Liu, Z. Zhang, L. He, and S. He, "Improving physical layer security for multi-UAV systems against hybrid wireless attacks," *IEEE Trans. Veh. Technol.*, vol. 73, no. 5, pp. 7034–7048, May 2024.
- [11] Y. Wang, Z. Su, Q. Xu, R. Li, T. H. Luan, and P. Wang, "A secure and intelligent data sharing scheme for UAV-assisted disaster rescue," *IEEE/ACM Trans. Networking*, vol. 31, no. 6, pp. 2422–2438, Dec. 2023.
- [12] Y. Wu, Z. Jia, Q. Wu, and Z. Lu, "Adaptive qoe-aware sfc orchestration in uav networks: A deep reinforcement learning approach," *IEEE Trans. Network Sci. Eng.*, vol. 11, no. 6, pp. 6052–6065, Aug. 2024.
- [13] Z. Wang, S. Li, E. J. Knoblock, H. Li, and R. D. Apaza, "Delay sensitive routing in an aerial and terrestrial hybrid wireless network via multi-agent reinforcement learning," in *Proc. IEEE Glob. Commun. Conf.*, Cape Town, South Africa, Dec. 2024, pp. 1497–1502.
- [14] Y. Lyu, H. Hu, R. Fan, Z. Liu, J. An, and S. Mao, "Dynamic routing for integrated satellite-terrestrial networks: A constrained multi-agent reinforcement learning approach," *IEEE J. Sel. Areas Commun.*, vol. 42, no. 5, pp. 1204–1218, May 2024.
- [15] H. Zhang, H. Tang, Y. Hu, X. Wei, C. Wu, W. Ding, and X.-P. Zhang, "Heterogeneous mean-field multi-agent reinforcement learning for communication routing selection in SAGI-net," in *Proc. IEEE 96th Veh. Technol. Conf. (VTC-Fall)*, London, United Kingdom, Sep. 2022.
- [16] Y. Chen, N. Zhao, Z. Ding, and M.-S. Alouini, "Multiple UAVs as relays: Multi-hop single link versus multiple dual-hop links," *IEEE Trans. Wireless Commun.*, vol. 17, no. 9, pp. 6348–6359, Sep. 2018.
- [17] G. Lancia and P. Serafini, *Compact Extended Linear Programming Models*. Cham, Switzerland: Springer, 2018.
- [18] H. Van Hasselt, A. Guez, and D. Silver, "Deep reinforcement learning with double Q-learning," in *Proc. 13th AAAI Conf. Artif. Intell.*, vol. 30, no. 1, Phoenix, Arizona, Feb. 2016, pp. 2094–2100.
- [19] Z. Jia, Q. Wu, C. Dong, C. Yuen, and Z. Han, "Hierarchical aerial computing for Internet of things via cooperation of HAPs and UAVs," *IEEE Internet Things J.*, vol. 10, no. 7, pp. 5676–5688, Apr. 2023.